Comparative study on the rheological properties and tablettability of various APIs and their composites with titatane nanotubes

Barbara Sipos[a], Géza Regdon jr.[a], Zoltán Kónya[b,c], Klára Pintye-Hódi[a], Tamás Sovány[a]*

[a]University of Szeged, Institute of Pharmaceutical Technology and Regulatory Affairs, Eötvös u. 6., H-6720, Szeged, Hungary

[b]University of Szeged, Department of Applied and Environmental Chemistry, Rerrich Béla tér 1., H-6720, Szeged, Hungary

[c]Hungarian Academy of Sciences-University of Szeged, Reaction Kinetics and Surface Chemistry Research Group, Rerrich Béla tér 1, H-6720, Szeged, Hungary

* Corresponding author: Tamás Sovány

Fax: +36-62-545571, Tel.: +36-62-545576, E-mail: t.sovany@pharm.u-szeged.hu

1. Introduction

Titanate nanotubes (TNT) are newly explored and promising nanomaterials for a wide range of medical applications. Among others, they show aptness to be used as radiosensitizer agents in radiotherapy [1], biocompatible biosensors [2] or cell viability and proliferation enhancing materials for orthopaedic and periodontal use [3, 4]. Besides, TNTs proved their capacity of being loaded with various active pharmaceutical ingredients (API) and therefore came into focus of pharmaceutical research as carrier materials [5, 6].

Based on the experimental results, drug loaded TNTs may provide development in many issues of pharmaceutical sciences. On the one hand, TNTs carrying nano-sized APIs may overcome fundamental difficulties related to the formulation and manufacturing of nanocrystalline active substances, which may show an unavoidable tendency to autoaggregation, thereby worsening their physicochemical properties and setting a limit to their commercialization. On the other hand, TNTs show an ability to achieve targeted drug delivery and controlled drug release, offering to put new and modern medical therapies into practice [7, 8]. From this aspect, the outstanding mechanical properties of TNTs may help to overcome formulation problems of other nanocarriers such as dendrimers, micelles, liposomes, etc., which are available on the market, but their large-scale manufacturing, stabilization as well as their processing into solid dosage forms require great efforts [9]. The present study aims to investigate the suitability of hydrothermally synthesized TNTs for the improvement of the processing of nano-sized APIs into solid dosage forms with direct compression method.

The structure of a tablet is influenced by many parameters, such as the physicochemical properties of the compressed materials, the type of the tablet press, the applied

compression force, etc. [10]. When focusing on the materials, the understanding of the behaviour of the compressed substances is essential for the commercial scale manufacturing of tablets. In order to reveal the tablettability of hydrothermally synthesized TNTs and estimate their influence on the rheological properties of APIs, which is a completely new field in pharmaceutical research, a competitive study was performed involving four APIs and their 1:1 ratio composites formed with TNTs. By using an instrumented tableting machine, the monitoring of the compression cycle is feasible and with the help of statistical models flowability, particle rearrangement and compressibility of the compressed materials are possible to be determined [11, 12]. In the present study the Kawakita-Lüdde and Walker compression models were applied to estimate the compressibility characteristics and the deformation mechanism of the API and API-TNT composite containing powder mixtures. The widely used Kawakita-Lüdde model [13] describes the volume reduction of the powder at a given compression pressure as a function of the pressure and therefore makes the analysis of particle rearrangement and compactibility possible. However, it does not give much information about the deformation mechanism of the powders, thus it is necessary to complement the analysis with another model. The Walker model [14], which expresses the volume reduction corresponding to a one-decade change in pressure, allows the characterisation of powder compressibility and therefore completes the Kawakita equation perfectly. Although the calculated parameters can serve to predict the post-compressional properties, tablets were investigated thoroughly in order to better understand the effects of TNT composite formation on tablet properties.

2. Materials and methods

2.1. Materials

Diltiazem hydrochloride (DiltHCl), diclofenac sodium (DicNa), atenolol (ATN) and hydrochlorothiazide (HCT) were kindly supported by Sanofi-Aventis PLC, Egis Pharmaceuticals PLC, TEVA Pharmaceuticals PLC and Gedeon Richter PLC, respectively. The following 1:1 ratio of active pharmaceutical ingredient (API)-hydrothermally synthesized titanate nanotube (TNT) composites were produced by the University of Szeged, Department of Applied and Environmental Chemistry: diltiazem hydrochloride-TNT (DiltTi), diclofenac sodium-TNT (DicTi), atenolol-TNT (ATNTi), hydrochlorothiazide-TNT (HCTTi). Excipients for tableting were Avicel PH 112 (FMC Biopolymer Inc., USA), Tablettose 70 (Meggle Pharma GbbH, Germany), talc and magnesium stearate.

2.2. Preformulation study

The flowing properties of the APIs and the API-TNT composites were examined by a software-controlled PTG-1 (Pharma Test Apparatebau AG, Germany) powder rheological tester. A stainless-steel funnel with a 10-mm-diameter outlet nozzle was filled with 100 ml of bulk powder and the powder flow was detected by IR sensors. The equipment measured the flow time and calculated the angle of repose of the powder heap.

Densification studies were performed for the APIs and the composites with a STAV 2003 Stampfvolumeter (Engelsmann AG., Germany). 250 ml of powder was put into a graduated cylinder taking care that the powder does not pack. This volume served to calculate the bulk density. The powder in the cylinder was mechanically tapped by the apparatus at a speed of 1/sec until no further decrease in volume could be observed or until tap number 1250 was reached. The volume of the densified powder was used to

calculate the tap density. The Hausner Ratio (Eq. (1)) and Compressibility Index (Eq. (2)) values of the samples were determined as follows:

Hausner Ratio $=\rho T/\rho B$ (1)

Compressibility Index = **[**$(\rho T - \rho B)/\rho T$**)] * 100(%)** (2)

where ρT is the tap density and ρB is the bulk density of the powder in **g/cm^3**.The evaluation of the results was based on the USP scale of flowability **[15].**

In order to determine the porosity of the APIs and the composites, the pycnometric volume of the powders was measured with a Quantachrome Helium Multipycnometer (Quantachrome GmbH, Germany). The porosity was calculated by applying Eq. (3):

ε = [1 - ($\rho B/\rho P$**)] * 100** **(3)**

where ε is the porosity (%), ρT **is the bulk density and** ρP **is the pycnometric density of the powder in g/cm^3.**

2.3. Tableting

Tablets containing APIs and API-TNT composites were formulated. The compositions of the tablets **displayed in Table 1. were designed for constant tablet weight (300 mg) and quantity of API (50 mg) in order to respect the therapeutic goals and be able to compare the API and API-TNT tablets according to the pharmaceutical requirements.**

The powders were mixed with a Turbula (Willy A. Bachofen Maschienenfabrik, Switzerland) mixer at 50 rpm for 8 minutes without magnesium-stearate and for 2

minutes more with it. The weight of the tablets was designed to be about 300 mg. The tablets were produced by the direct compression method with a Korsch EK0 (E. Korsch Maschienenfabrik GmbH, Germany) eccentric tablet press, instrumented with strain gauges and a displacement transducer. 10-mm-diameter flat punches were applied with a compression force of 5.0, 7.5, 10.0, 12.5 and 15.0 kN for all the compositions.

2.4. Compaction properties

The compaction properties of the powder mixtures (Table 1.) were estimated according to the out-of-the-die method using the Kawakita and Walker models.

The Kawakita equation (Eq. (4)) was used to study the particle rearrangement of the powder mixtures during the compression:

$$P/C = P/a + 1/ab \quad (4)$$

where *P* is the applied pressure **in MPa**, *C* is the degree of the volume reduction and *a* and *b* are constants. The degree of volume reduction is expressed by Eq. (5):

$$C = (V_0-V)/V_0 \quad (5)$$

where V_0 is the initial volume of the powder bed and *V* is the volume of the powder bed at the applied pressure **in mm^3**.

Constant *a* gives an indication of the initial porosity of the sample. Its higher value presumes the loose packing of the powder in the die before compression. Constant *1/b* describes the pressure which is needed to reduce the powder bed volume by 50%. Higher coefficient *1/b* implies higher cohesive energy of interaction, which shows up as a hindered particle rearrangement.

The compressibility of the powder mixtures was investigated using the Walker (1923) equations (Eq. (6) and (7)):

$$\log P = -LV + C_1 \quad (6)$$

138 $100V = -W \log P + C$ (7)

139 where *P* is the applied pressure **in MPa**, *L* is the pressing modulus which reflects the
140 volume reduction at a given pressure, *V* is the relative volume, *W* is the Walker
141 coefficient which gives information about the volume reduction corresponding to one-
142 decade change in the pressure, and *C* and C_1 are constants. The relative volume is
143 expressed by Eq. (8):

144 V'/V_0 (8)

145 where *V'* is the volume at the applied pressure and V_0 is the initial volume of the powder
146 bed **in mm^3**.

147

148 2.5. Post-compressional properties

149 The mass, the thickness and the diameter of the prepared tablets were investigated with
150 a Kraemer UTS-50 **(**Charles Ischi AG, Switzerland**)** tablet testing system right after the
151 production and one week later in order to follow the changes in the geometrical
152 parameters. 20 numbered tablets of each composition and compression force were
153 characterized. The parameters above served to calculate the apparent density of the
154 tablets. **In addition to the apparent density, the study was completed with**
155 **pycnometric density measurements allowing the determination of tablet porosity**
156 **(see the applied method under Section 2.2.)**
157 The breaking strength of the tablets was studied with a Heberlein 2E/205 tablet hardness
158 tester (Heberlein AG, Switzerland), measuring 10 tablets per composition per
159 compression pressure. In addition, the tensile strength of the tablets was calculated
160 using the following equation (Eq. (9)):

161 $\sigma = 2F/(\pi * d * h)$ (9)

where σ is the tensile strength **in N**, F is the breaking force in N, d is the diameter and h is the height of the tablet **in mm**.

The texture of the prepared tablets was studied by taking Scanning Electron Micrographs of the surface, while their breaking surface was examined with a Hitachi S4700 (Hitachi Ltd., Japan) scanning electron microscope. The tablets were stuck to a double-sided carbon adhesive tape and a conductive golden layer was deployed with the use a sputter apparatus (Polaron Ltd., UK). The measurements were performed at a magnification of 100-500, applying 10.0 kV of electron energy and 1.3-13 MPa of air pressure.

The disintegration of the prepared tablets was investigated **in distilled water** with an Erweka ZT71 (Erweka GmbH, Germany) disintegration tester apparatus according to the criteria of the Eur. Pharmacopoeia **[16].**

The drug release from the tablets was determined by an Erweka DT700 (Erweka GmbH, Germany) dissolution tester, using the USP II method [17]. The dissolution was tested at 37 °C, with pH 6.8 phosphate buffer as a dissolution medium. The 5-ml aliquots were taken after 3, 5, 10, 15, 30, 60, 90, 120 minutes. The dissolved drug (μg/ml) was defined with a ThermoScientific GENESYS 10S UV-VIS spectrophotometer (Thermo Fisher Scientific Ltd., USA).

3. Results and discussion

3.1. Preformulational properties of the APIs and the API-TNT composites

Within the preformulation studies, the determination of the flow properties, the Hausner Ratio and Compressibility Index values **and the porosity** of the samples was put into focus (Table 2.). The results showed uniformity in that the composites displayed

preferable flow properties compared to the pure APIs, irrespective of the incorporated API.

The measurements revealed that the APIs have extremely poor flow properties. In contrast, favourable flowability was observed for the pure TNTs. As concerns the composites, the results are not consonant, the incorporation of DiltHCl and DicNa induced better (measurable) flow time, while the composite formation of ATN and HCT did not result in measurable flow time. This can be explained by the partially feasible incorporation of ATN and HCT into TNTs [18]. Therefore, as ATNTi and HCTTi products contain individual API crystals, the flowability improving effect of TNTs decreases or completely lags behind.

The investigation of the particle rearrangement revealed an exponential-type rearrangement profile for all the samples **(Fig.1).** Regarding the calculated Hausner Ratio and Compressibility Index values, it is clearly visible that all the APIs reached an upper range of the USP scale of flowability **[15]** by the incorporation. The flowability of the composites varies between those of the component materials, which was expected based on the fact that the APIs are located not only in the inner parts of TNTs but on their surface as well [18]. The rate of the flowability improvement probably depends on the ratio of the surface coverage.

The results of the pycnometric volume measurements confirmed that TNTs possess notably high pycnometric density and high porosity, which was expected due to the tubular structure and the great number of interparticular pores between the nanosized particles. Accordingly, the porosity of the composites is also greater than that of the pure APIs: this phenomenon was more expressed for DiltTi and DicTi, where the drug incorporation was complete, and less (or not) expressed for the partially incorporated ATNTi and HCTTi products. It is also notable that HCTTi,

where TNTs are attached to the surface of the HCT particles [18], exhibits slightly decreased porosity, which may be due to the decreasing number of interparticular pores.

3.2. Compaction properties of the API and API-TNT containing powder mixtures

The tablettability of the powder mixtures was thoroughly investigated by using an instrumented tablet press.

Knowing the degree of volume reduction under pressure, the particle rearrangement of the powder mixtures was studied by using the Kawakita model. The results of the analysis were plotted; the graphs of the DiltHCl and DiltTi tablets are presented in Fig. 2. The data fit the Kawakita model well with a R^2 being at least 0.998. Constants *a* and *1/b*, which were obtained from the graphs, are displayed in Table 3.

The values of constant *a*, which give information about the rearrangement of the powders, are very similar for all the samples. Although the preformulation studies presumed lower constant *a* values for the composite containing compositions, no remarkable differences could be noticed either between the four API tablet compositions or between the API and the related API-TNT tablet compositions. This result confirms the selection of an appropriate excipient profile for the tablets, resulting in powder mixtures with nearly the same flow properties. However, the fact that the compositions of the composites contain proportionally less excipient than those of the APIs implies the better flowability of the composites.

The values of constant *1/b*, which correlate with the cohesiveness, showed important differences between the API and API-TNT tablet compositions. Based on the several times higher *1/b* values of the composite containing powders, it is clear that the composite content requires much higher energy to reduce the volume of the powder to

half of the original. The low*1/b* values can be explained by the fast collapse of the powders in the die, supporting our visual observations made during the preformulation studies. In contrast, powders with a high *1/b* value exhibit continuous densification under increasing load. It can be seen that the relation between the value of constant *a* of the HCT and the HCTTi tablet compositions is different, and the HCTTi containing powder mixtures have a lower *1/b* value than the HCT tablet composition. In order to make this exceptional behaviour clear, the structural properties of the HCTTi product have to be taken into consideration. As it was already mentioned, the incorporation of HCT into TNTs was not completely successful, resulting in a product which, besides the aggregated composites, contains HCT crystals covered with TNTs [18]. Owing to the surface coverage, the HCTTi product displays higher surface free energy than the pure HCT, therefore it shows superior adhesivity as well. For this reason, instead of improving compactibility, the HCTTi product generates an unfavourable particle rearrangement, showing an even worse compactibility profile than the pure API itself. The compressibility of the compositions was examined by applying the Walker model. From the plotted graphs (the graphs of DiltHCl and DiltTi tablets are shown in Fig. 3 and 4) coefficients *L* and *W* were defined. The data are presented in Table 3. According to the results, coefficient *L*, also called pressing modulus, appeared to be lower for the composite containing compositions, reflecting their higher volume reduction at a given pressure compared to the tablet compositions containing pure API. This behaviour is supported by the preformulation studies, during which the composites revealed higher density than the APIs, and also by the fact that the composite formation results in smaller surface free energy [18]. The results of HCT and HCTTi tablet powder mixtures showed up again oppositely, thus the HCTTi containing composition

displayed a higher coefficient *L* value. This result is in perfect accordance with our conception described above.

The obtained Walker coefficient values, which refer to the irreversible compressibility of the powders, correspond with the results discussed so far. The higher values of coefficient *W* shown by the composite containing compositions hint at plastic deformation and better tableting properties. In contrast, the smaller *W* values of tablet compositions containing pure API mark an extended densification maximum due to the high elastic recovery of the crystalline APIs. In this case again, the HCTTi composite containing powder mixture showed opposing behaviour as compared to the other API-TNT tablet compositions, confirming the above-mentioned negative effect of the unsuccessful composite formation.

Overall, it can be concluded that the incorporation of drugs into TNTs is advantageous and results in more ideal compaction behaviour. However, it is also important to remark that a partially successful composite formation may affect the compaction properties negatively, therefore the appropriate incorporation process plays a key role in this issue.

3.3. Post-compressional properties of the API and API-TNT tablets

The measurements of the geometric parameters allowed us to define the apparent density of the tablets right after the compression and one week later as well. The results are summarized in Table 4.

Based on the data, it can be stated that the tablet density generally increases with the compression force. The only exception was shown by the ATN tablets, where the density measured right after compression decreased with the increase of the compression force. This phenomenon can be explained by the strong elasticity of ATN, which results in a rising elastic recovery with the increase of the compression force.

This conception is supported by the low value of coefficient *W* received from the Walker analysis (Table 3.). **Nevertheless, the density values measured after one-week storage show that the bonds in the ATN containing tablets undergo a considerably high consolidation during the first period of storage, which may also be observed in the case of other elastic systems [19].** It is also noteworthy that this phenomenon did not appear for the ATNTi tablets, which shows the positive effect of TNTs on elastic recovery.

It can also be established from the data that the apparent density of the API-TNT tablets is higher than that of the API tablets for all the investigated compression forces. However, in the case of DicNa and DicTi tablets this statement is relevant only at higher compression forces, which supports the good rearrangement and compressibility properties of DicNa seen in Table 3. Nevertheless, it can be concluded that the presence of TNTs generally increases the apparent tablet density.

It is also necessary to consider the post-compressional apparent density changes as they can provide further information about the processability of the APIs and their composites. The density of the DiltHCl tablets decreased in time at each compression force, while the density of the DicNa, ATN and HCT tablets increased during the one-week storage. The decrease in density is probably due to the release of the stored stress by the tablet by increasing its volume, while the increase of tablet density is probably the result of the consolidating bonding forces. Regarding the API-TNT tablets, in the case of DiltTi and DicTi the density did not change at lower compression forces and only barely decreased beyond 10.0kN in time. These results support the plastic deformation of these composite containing compositions inducing stable tablet density at low compression forces and only slight changes in density at high compression pressure. On the other hand, the apparent density of the ATNTi and HCTTi tablets was

noticed to increase during the one-week storage at all compression forces. These results showing similarity to those of the ATN and HCT tablets certainly originate in the incomplete incorporation of these materials into TNTs. Furthermore, in the case of the HCTTi tablets it was also predictable based on the compaction studies.

As regards the true density and the porosity of the tablets (Table 5.), those containing composites showed higher true density than API tablets, which is in accordance with the presented apparent densities as well as with the expectations built on the powder porosities shown in Table 2. The porosity of the tablets, which constantly decreased with the increase of the compression pressure, exhibits considerable differences with regard to the compressibility and the texture of the compositions. According to the preformulation results, all the composites have higher porosity than the pure APIs, due to the tubular structure of TNTs. This difference is clearly visible also for tablets prepared from composites which exhibit poorer compressibility (DicTi and ATNTi), while tablets prepared from DiltTi, which showed superior compressibility, have lower porosity than the corresponding DiltHCl tablets at all compression forces. A slight decrease of porosity may also be observed for the HCTTi tablets, but this can be due to the unique structure of the composite and not to the good compressibility of the composition.

The forces required to break the tablets and the calculated tensile strength values are displayed in Table 6.

As expected, the breaking strength increases with the compression force in all the cases. Based on the results, it is outstanding that the breaking strength of the API-TNT tablets is much superior to that of the API tablets at all compression forces. Moreover, in consonance with the results of the compaction measurements, the API-TNT tablets

display a greater increase in breaking strength between 5.0 and 15.0 kN compression force than the API tablets. According to the data, the less influence of the incorporation on the breaking strength was observed for DicNa, where a difference of 3.0 N could only be detected in the breaking strength of DicNa and DicTi tablets at 5.0 kN compression force. Although this difference slightly increased with the compression force, it was not remarkable at 15.0 kN either. This observation is in agreement with the results of the apparent density measurements. Comparing the four APIs, HCT (and therefore HCTTi) tablets showed the biggest breaking strengths at each compression force. In accordance with the high apparent density values displayed in Table 4., these results prove their greater hardness compared to the other samples.

The disintegration time of the API and API-TNT tablets was investigated in order to reveal the effect of the composite formation on the disintegration and therefore its impact on drug dissolution. The results of the measurements are shown in Table 6.

As expected, the disintegration time rose with the compression pressure in all the cases. When comparing the API and API-TNT tablets, it can be stated that the disintegration of the composite containing tablets is slower at each investigated compression pressure. The superior disintegration times of the API-TNT tablets refer to their greater hardness, confirming the findings of the above post-compression studies.

The most considerable effect of the incorporation on the disintegration time was seen for the ATN tablets as a result of the important difference in strength observed between the ATN and ATNTi tablets. It is noteworthy that the partial incorporation of HCT is clearly reflected in the results: the HCT and HCTTi tablets show similar disintegration time values. It is also interesting to note that despite their high hardness and apparent density, the HCT and HCTTi tablets disintegrate very quickly and, in contrast with the other compositions, their disintegration is less dependent on the compression pressure.

The scanning electron micrographs of the tablets (Fig. 5.) support the results of the compressibility studies, according to which the HCT and HCTTi tablets go through a considerably higher densification already at lower compression forces, resulting in smaller porosity. The SEM pictures also reveal that the irregular densification may be due to the fragmentation of the HCT particles, which may also be an explanation for the fast disintegration process. The water penetrating into the microfractures (marked with white arrows) of the HCT particles disrupts the fractures and the released energy enhances the disintegration process.

The results of the dissolution tests are presented in Fig. 6. In general, slower drug release may be observed from the API-TNT tablets than from the related API tablets in all the cases. This may be explained by the slower disintegration, due to the higher breaking strength and density of these tablets, independently from their porosity. This may support the conclusion that the observed porosity differences between the APIs and the composites are due to the tubular structure of TNTs and not to the looser tablet skeleton. It is important to note that the occurrence of strong interactions may also change the kinetics of the drug release, as observed in the case of DicNa, where the first order drug dissolution from the DicNa tablets changed to prolonged dissolution based on Korsmeyer-Peppas kinetics from the DicTi tablets. In accordance with the expectations, the speed of dissolution decreased with the increase of the compression force in the case of the API and API-TNT tablets as well. However, it could be seen that this slowing down of dissolution was more intense for the API-TNT tablets, confirming the especially good compressibility and compactibility of the composites.

4. Conclusion

The present study aimed to determine the effect of 1:1 ratio API-TNT composite formation on the tablettability of the incorporated API. Four different composite products were used to obtain reliable results.

The preformulation measurements revealed that the composite formation with TNTs highly improved the extremely poor flowability of the APIs. This positive effect of TNTs on powder rheology was proved for all the investigated APIs, indicating promising opportunities for developing drug processability with the use of TNTs. However, the rate of flowability improvement was seen to be dependent on the efficiency of the incorporation process; ATNTi and HCTTi showed slighter flowability improvement.

When comparing the compaction properties of the API and API-TNT tablets, it was seen that the composite formation resulted in better compactibility, showing higher volume reduction at a given compression pressure. Furthermore, drug incorporation into TNTs hindered the elastic recovery of the APIs and led to plastic deformation. These results confirmed the great advantage of composite formation for manufacturing tablets with direct compression. On the other hand, the measurements also revealed that inappropriate incorporation may also affect the compaction behaviour of the API negatively, as observed for HCT. Accordingly, the successfulness of the incorporation is considered to be the key factor of the tablettability improving effect of TNTs.

In accordance with the more ideal compaction behaviour, the API-TNT tablets showed better post-compressional properties than the tablets containing pure APIs, displaying higher apparent density, superior breaking strength and slower disintegration at all the applied compression forces. The greater strength of the API-TNT tablets compared to that of the pure APIs was observed for all the APIs without reference to the efficacy of the incorporation.

Overall, the present work revealed that the appropriate incorporation of APIs into TNTs highly improves their tablettability and results in tablets with favourable mechanical properties. Accordingly, it can be concluded that hydrothermally synthesized TNTs can advantageously be used as drug carriers in the manufacturing of tablets with direct compression.

Acknowledgements

The authors would like to thank Péter Kása jr. for taking the SEM pictures.

Conflict of Interest

The authors declare that there is no conflict of interest regarding the publication of this paper.

References

[1] C. Mirjolet, A. Papa, G. Créhange, O. Raguin, C. Seignez, C. Paul, G. Truc, P. Maingon, N. Millot, The radiosensitization effect of titanate nanotubes as a new tool in radiation therapy for glioblastoma: A proof-of-concept, Radiotherapy and Oncology 108 (2013) 136-142.

[2] R. Zhao, X.Liu, J. Zhang, J. Zhu, D. K. Y. Wong, Enhancing direct electron transfer of glucose oxidase using a gold nanoparticle/titanate nanotube nanocomposite on a biosensor, Electrochimica Acta 163 (2015) 64–70.

[3] S. Beke, R. Barenghi, B. Farkas, I. Romano, L. Kőrösi, S. Scaglione, F. Brandi, Improved cell activity on biodegradable photopolymer scaffolds using titanate nanotube coatings, Materials Science and Engineering: C 44 (2014) 38-43.

[4] E. Kato, K. Sakurai, M. Yamada, Periodontal-like gingival connective tissue attachment on titanium surface with nano-ordered spikes and pores created by alkali-heat treatment, Dental Materials 31 (2015) 116–130.

[5] K. Indira, U. KamachiMudalib, N. Rajendran, In vitro bioactivity and corrosion resistance of Zr incorporated TiO2 nanotube arrays for orthopaedic applications, Applied Surface Science 316 (2014) 264–275.

[6] A. L. Doadrio, A. Conde, M. A. Arenas, J. M. Hernández-López, J. J. de Damborenea, C. Pérez-Jorge, J. Esteban, M. Vallet-Regí, Use of anodized titanium alloy as drug carrier: Ibuprofen as model of drug releasing, International Journal of Pharmaceutics 492 (2015) 207-12.

[7] Y. Zhang, L. Chen, C. Liu, X. Feng, L. Wei, L. Shao, Self-assembly chitosan/gelatin composite coating on icariin-modified TiO2 nanotubes for the regulation of osteoblast bioactivity, Materials & Design 92 (2016) 471-479.

[8] T. Kumeria, H. Mon, M. S.Aw, K. Gulati, A. Santos, H. J. Griesser, D. Losi, Advanced biopolymer-coated drug-releasing titania nanotubes (TNTs) implants with simultaneously enhanced osteoblast adhesion and antibacterial properties, Colloids and Surfaces B: Biointerfaces 130 (2015) 255–263.

[9] A. Elhissi, D. Phoenix, W. Ahmed, Some approaches to large-scale manufacturing of liposomes**,** Emerging Nanotechnologies for Manufacturing, second ed., William Andrew, 2015

[10] Ch. Mao. V. R. Thalladi, D. K. Kim, S. H. Ma, D. Edgren, S. Karaborni, Harnessing ordered mixing to enable direct-compression process for low-dose tablet manufacturing at production scale, Powder Technology 239 (2013) 290–299.

[11] T. Osamura,' Y. Takeuchi, R. Onodera, M. Kitamura, Y. Takahashi, K. Tahara, H. Takeuchi, Characterization of tableting properties measured with a multi-functional

compaction instrument for several pharmaceutical excipients and actual tablet formulations, International Journal of Pharmaceutics 510, Issue 1 (2016) 195–202.

[12] A. Hadadzadeh, M. A. Whitney, M. A. Wells, S. F. Corbin, Analysis of compressibility behavior and development of a plastic yield model for uniaxial die compaction of sponge titanium powder, Journal of Materials Processing Technology 243 (2017) 92–99.

[13]A. Persson, J. Nordström, G. Frenning, G. Alderborn, Compression analysis for assessment of pellet plasticity: Identification of reactant pores and comparison between Heckel, Kawakita, and Adams equations, Chemical Engineering Research and Design 110 (2016) 183–191.

[14] S. Mallick, Rearrangement of particle and compactibility, tabletability and compressibility of pharmaceutical powder: A rational approach, Journal of Scientific & Industrial Research 110 (2016) 183–191.

[15] United States Pharmacopeia Convention, Pharmacopeia and National Formulary (USP 29 – NF 24), General Chapters: <1174> POWDER FLOW, United States Pharmacopeia Convention, Inc., Rockville, MD, United States (2000), 3017.

[16] Council of Europe, European Pharmacopoeia, 5th ed. Main volume 5.0,2.9.1. Disintegration of tablets and capsules, Council of Europe, Strasbourg (2004) 225-227.

[17] United States Pharmacopeia Convention, Pharmacopeia and National Formulary (USP 29 – NF 24), General Chapters: <711> DISSOLUTION, United States Pharmacopeia Convention, Inc., Rockville, MD, United States (2000) 2673.

[18] B. Sipos, K. Pintye-Hódi, Z. Kónya, A. Kelemen, G. Regdon jr., T. Sovány, Physicochemical characterisation and investigation of the bonding mechanisms of API-

titanate nanotube composites as new drug carrier systems, International Journal of Pharmaceutics 518 (2017) 119–129.

[19] I. Jójárt, A. Kelemen, P. Kása jr., K. Pintye-Hódi, Tracking of the post-compressional behaviour of chewing gum tablets, Composites Part B: Engineering, 49 (2013) Pages 1-5

Figure captions

Figure 1: Particle rearrangement profile of TNTs, APIs and API-TNT composites

Figure 2: Kawakita-Lüdde plot of DiltHCl and DiltTi containing powder mixtures

Figure 3: Walker W plot of DiltHCl and DiltTi containing powder mixtures

Figure 4: Walker L plot of DiltHCl and DiltTi containing powder mixtures

Figure5: SEM micrographs of tablets (DicTi 5kN tablet surface (a) and breaking surface (b); DicTi 15kN tablet surface (c), breaking surface (d); HCTTi 5 kN tablet surface (e), breaking surface (f); HCTTi 15 kN tablet surface (g), breaking surface (h))

Figure 6: Drug dissolution from API and API-TNT tablets compressed with 5.0, 7.5, 10.0, 12.5 and 15.0 kN in pH 6.8 phosphate buffer

***Graphical Abstract (for review)**

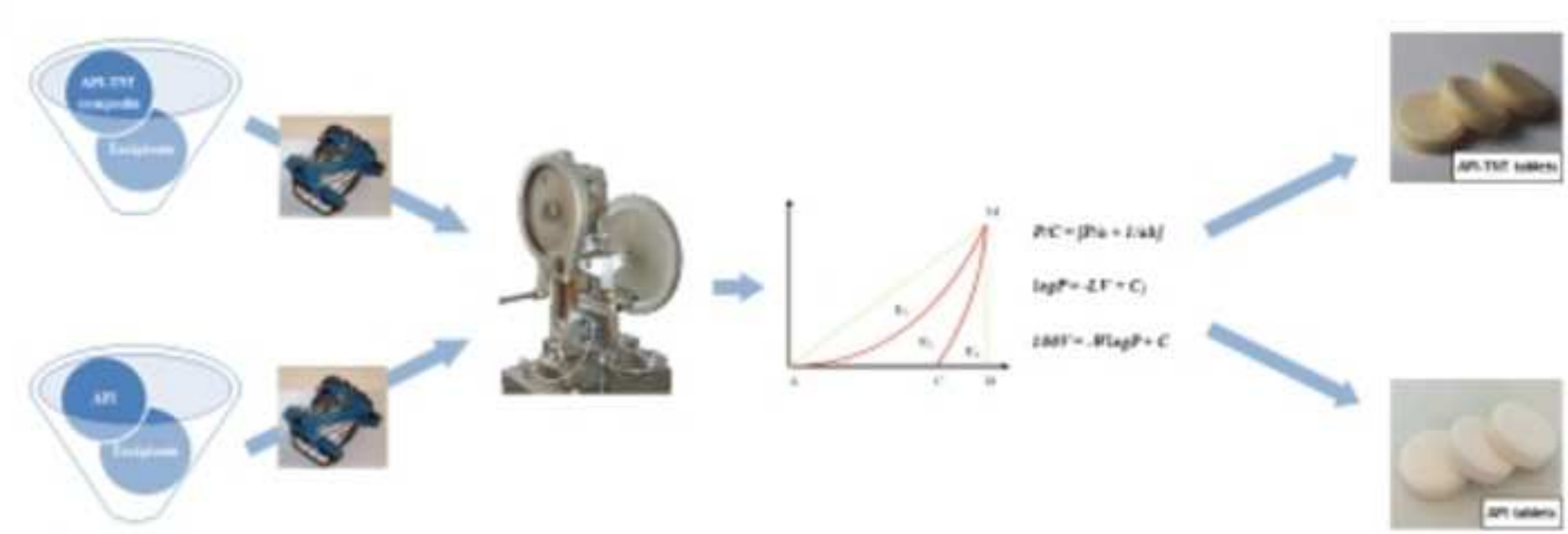

Figure(s)

Click here to download high resolution image

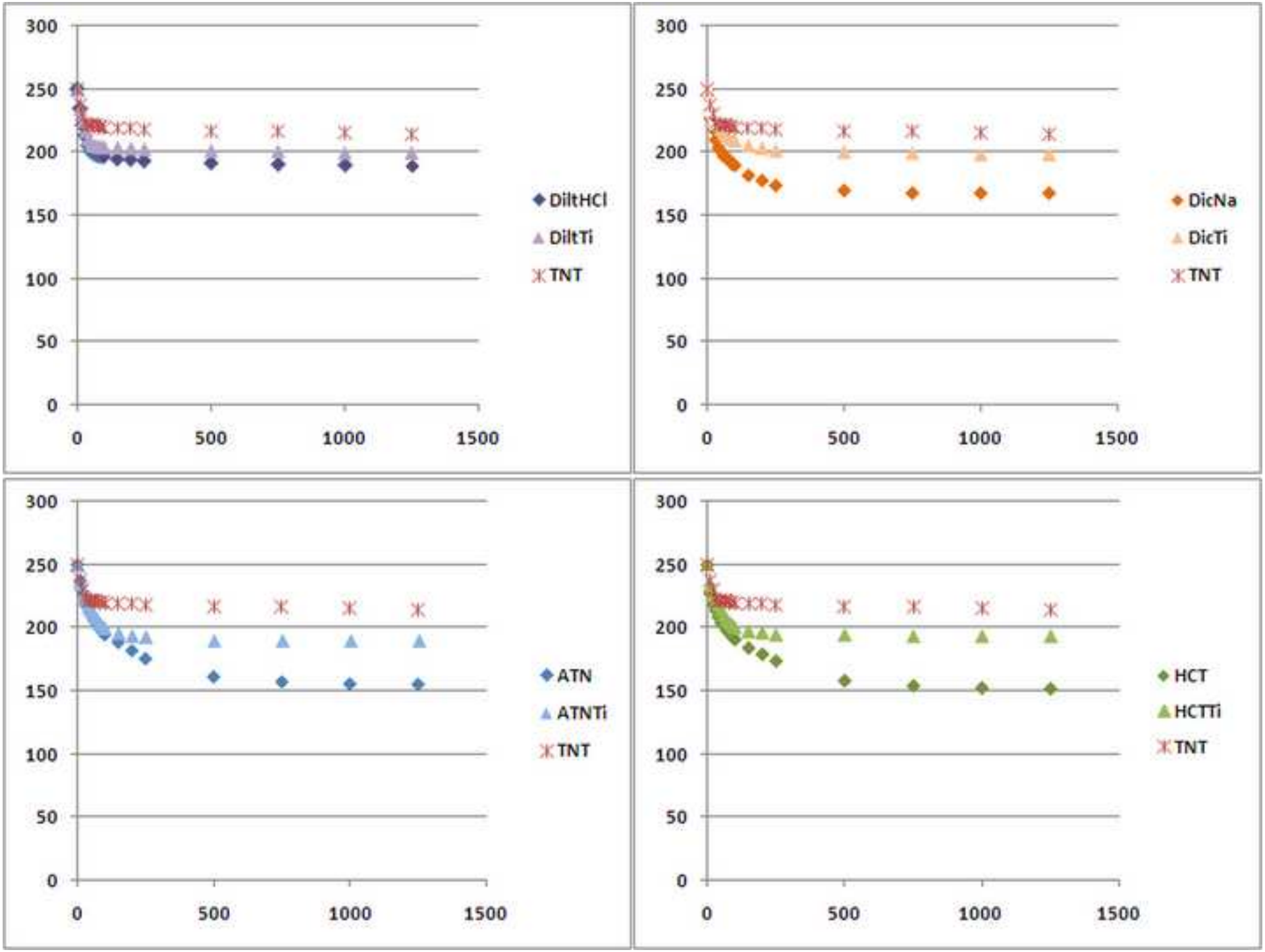

Figure(s)

Click here to download high resolution image

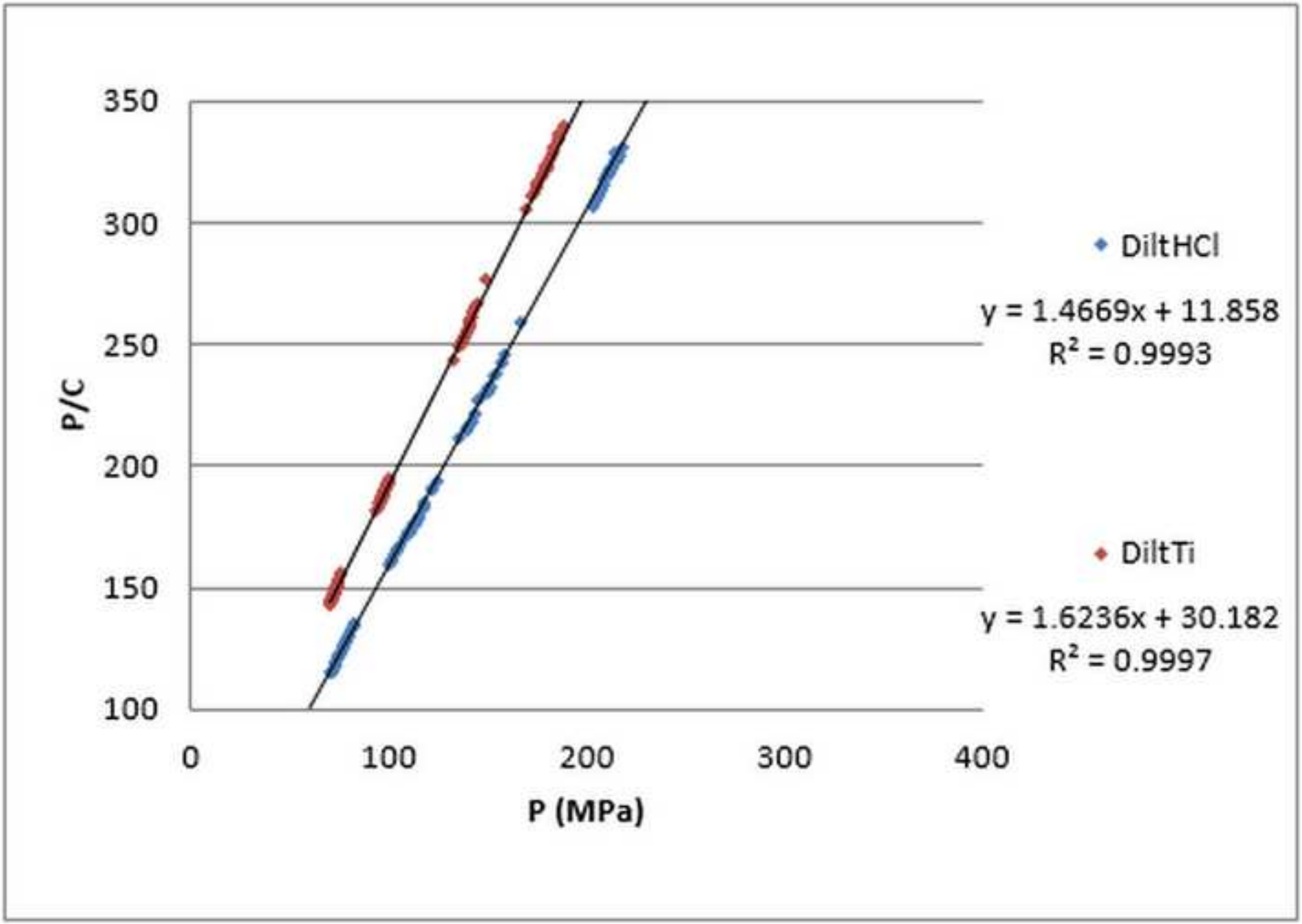

Figure(s)

Click here to download high resolution image

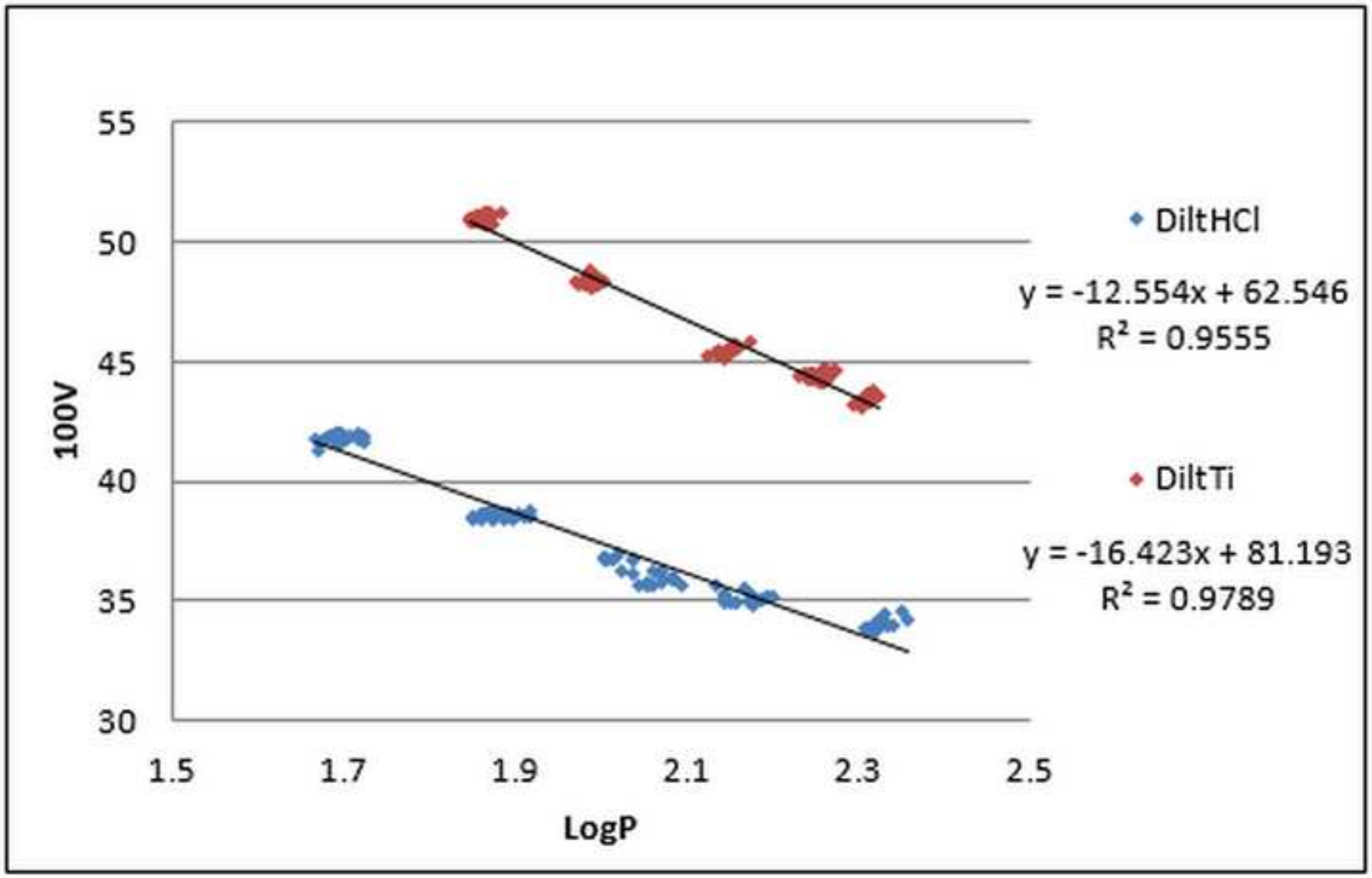

Figure(s)

Click here to download high resolution image

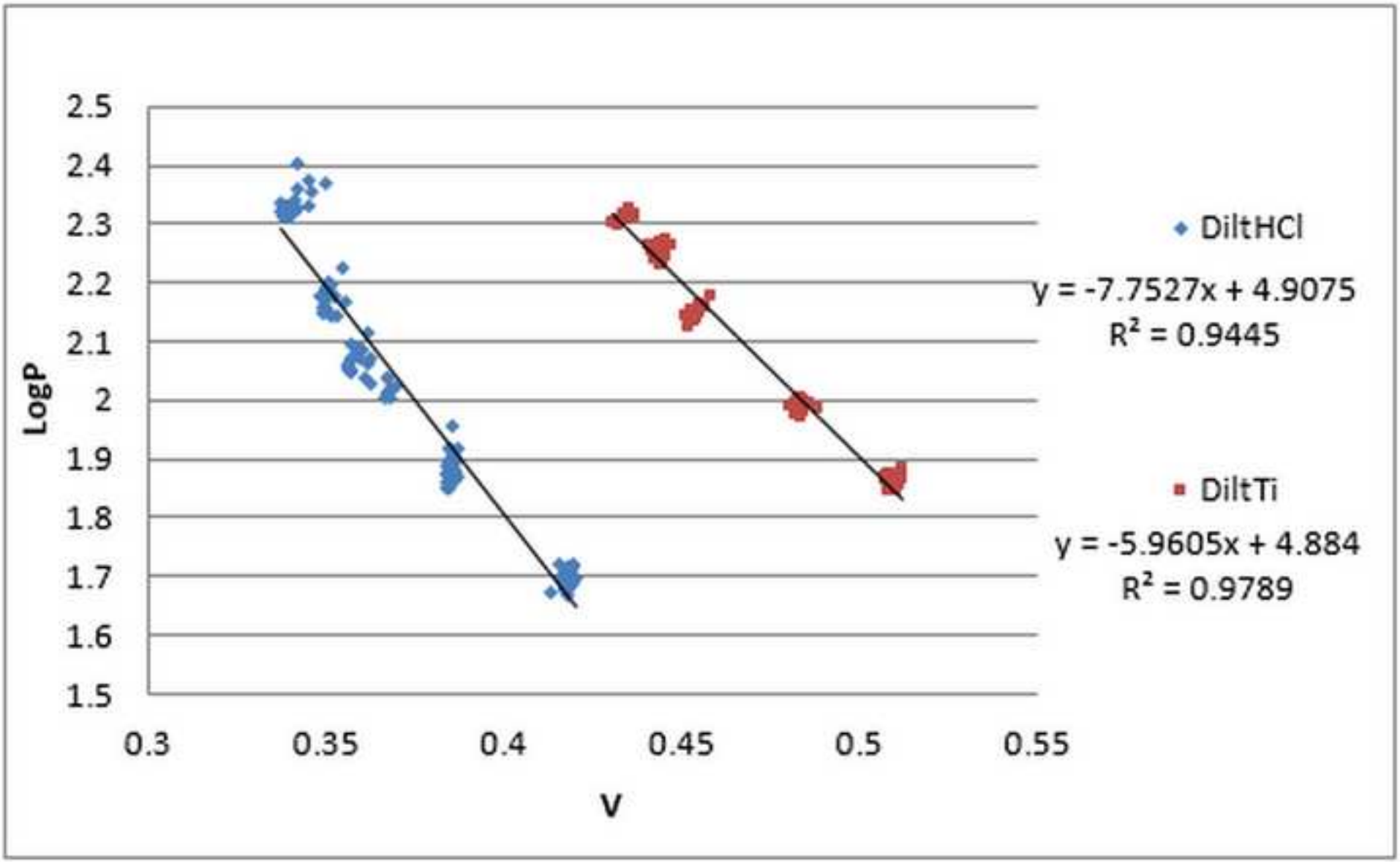

Figure(s)

Click here to download high resolution image

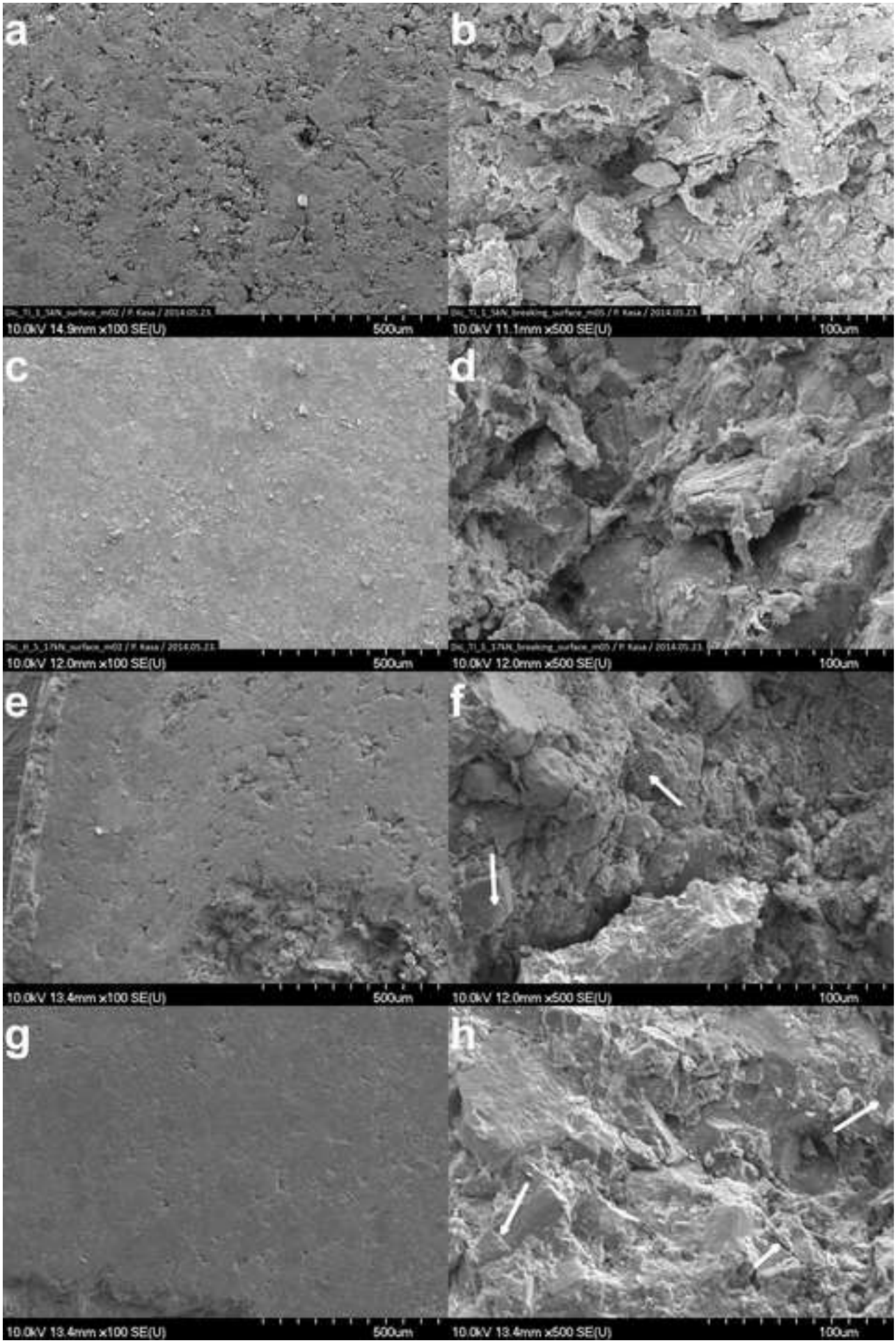

Figure(s)

Click here to download high resolution image

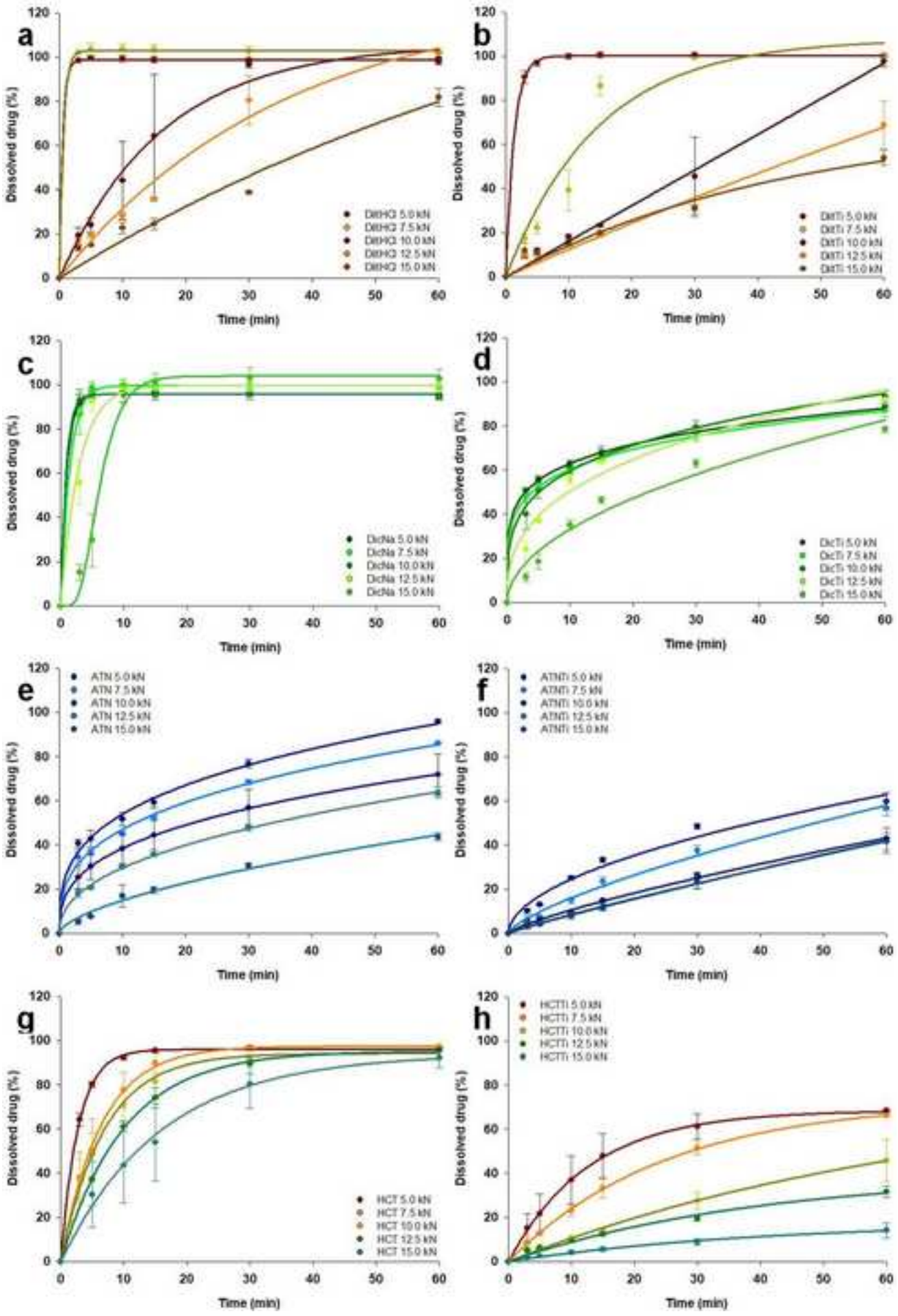

Table 1. Composition of API and API-TNT tablets

Materials	*API tablets*	*API-TNT tablets*
API	*16.7%*	-
API-TNT	-	*33.3%*
Avicel PH 112	*50.0%*	*39.5%*
Tablettose	*29.3%*	*23.2%*
Talc	*3.0%*	*3.0%*
Mg-stearate	*1.0%*	*1.0%*

Table 2. Preformulation results of the APIs and the API-TNT composites

Material	Flow time (sec)	Angle of repose (°)	Bulk density (g/cm^3)	Tapped density (g/cm^3)	Pycnometric density (g/cm^3)	Porosity (%)	Hausner Ratio	Compressibility Index (%)	Flowability (USP scale)
TNT	14.3	25.5	0.65	0.76	3.02	78.51	1.17	14.47	good
DiltHCl	n.m.	-	0.45	0.59	1.30	65.34	1.31	23.73	passable
DiltTi	16.5	28.2	0.51	0.64	1.78	71.39	1.25	20.31	fair
DicNa	n.m.	-	0.48	0.73	1.50	68.01	1.52	34.25	very poor
DicTi	6.3	28.4	0.55	0.68	1.97	72.05	1.24	19.12	fair
ATN	n.m.	-	0.3	0.48	1.21	75.16	1.6	37.5	very very poor
ATNTi	n.m.	-	0.38	0.49	1.64	76.81	1.29	22.45	passable
HCT	n.m.	-	0.46	0.76	1.69	72.72	1.65	39.47	very very poor
HCTTi	n.m.	-	0.61	0.76	2.17	71.94	1.25	19.74	fair

n.m.=not measurable

Table 3. Parameters calculated from Kawakita and Walker plots

Tablet	***a***	***1/b***	***L***	***W***
DiltHCl	0.68	8.03	7.9	11.59
DiltTi	0.62	18.63	5.93	16.49
DicNa	0.67	6.38	9.85	8.72
DicTi	0.68	13.53	6.64	14.73
ATN	0.64	5.94	13.56	4.04
ATNTi	0.65	17.61	8.47	9.43
HCT	0.61	14.32	12.89	7.01
HCTTi	0.68	6.04	17.76	2.49

Table 4. Apparent density of the API and API-TNT tablets determined right after the preparation and one week later

Pressing force (kN)	API				Composite			
	0 h		168 h		0 h		168 h	
	Apparent density	SD	Apparent density	SD	Apparent density	SD	Apparent density	SD
	DiltHCl				**DiltTi**			
5.0	1.09	0.01	1.06	0.01	1.23	0.01	1.23	0.00
7.5	1.18	0.01	1.15	0.01	1.30	0.00	1.30	0.00
10.0	1.25	0.01	1.23	0.01	1.35	0.02	1.35	0.01
12.5	1.29	0.01	1.27	0.01	1.40	0.01	1.39	0.00
15.0	1.30	0.07	1.28	0.08	1.42	0.00	1.40	0.00
	DicNa				**DicTi**			
5.0	1.16	0.01	1.16	0.01	1.16	0.00	1.16	0.01
7.5	1.23	0.02	1.26	0.02	1.23	0.01	1.23	0.02
10.0	1.27	0.01	1.32	0.02	1.32	0.00	1.32	0.00
12.5	1.30	0.01	1.35	0.02	1.36	0.01	1.35	0.02
15.0	1.34	0.01	1.40	0.01	1.42	0.00	1.40	0.04
	ATN				**ATNTi**			
5.0	1.11	0.01	1.25	0.01	1.15	0.01	1.31	0.01
7.5	1.04	0.01	1.28	0.01	1.20	0.01	1.37	0.00
10.0	1.01	0.01	1.28	0.01	1.23	0.01	1.40	0.01
12.5	0.93	0.00	1.30	0.01	1.24	0.01	1.42	0.01
15.0	0.92	0.01	1.32	0.01	1.25	0.02	1.43	0.01
	HCT				**HCTTI**			
5.0	1.03	0.01	1.28	0.01	1.17	0.00	1.39	0.01
7.5	1.07	0.01	1.33	0.01	1.20	0.01	1.42	0.00
10.0	1.09	0.03	1.39	0.01	1.26	0.00	1.48	0.01
12.5	1.11	0.00	1.40	0.00	1.31	0.00	1.48	0.01
15.0	1.12	0.00	1.41	0.00	1.37	0.00	1.52	0.00

Table 5. True density and porosity of the API and API-TNT tablets

Pressing force (kN)	True density (g/cm^3)	SD	Porosity (%)	SD	True density (g/cm^3)	SD	Porosity (%)	SD
	DiltHCl				**DiltTi**			
5.0	1.0517	0.0098	29.41	0.45	1.6336	0.0080	24.70	0.36
7.5	1.0517	0.0098	23.42	0.49	1.6336	0.0080	20.42	0.38
10.0	1.0517	0.0098	18.09	0.53	1.6336	0.0080	17.35	0.40
12.5	1.0517	0.0098	15.43	0.54	1.6336	0.0080	14.91	0.41
15.0	1.0517	0.0098	14.76	0.55	1.6336	0.0080	14.29	0.41
	DicNa				**DicTi**			
5.0	1.5426	0.0065	24.80	0.31	1.6685	0.0151	30.47	0.62
7.5	1.5426	0.0065	18.31	0.34	1.6685	0.0151	26.27	0.66
10.0	1.5426	0.0065	14.42	0.36	1.6685	0.0151	20.88	0.71
12.5	1.5426	0.0065	12.48	0.37	1.6685	0.0151	19.08	0.73
15.0	1.5426	0.0065	9.243	0.38	1.6685	0.0151	16.08	0.75
	ATN				**ATNTi**			
5.0	1.4721	0.0045	15.08	0.26	1.5953	0.0043	17.88	0.21
7.5	1.4721	0.0045	13.04	0.26	1.5953	0.0043	14.11	0.22
10.0	1.4721	0.0045	13.04	0.26	1.5953	0.0043	12.23	0.23
12.5	1.4721	0.0045	11.68	0.27	1.5953	0.0043	10.98	0.23
15.0	1.4721	0.0045	10.33	0.27	1.5953	0.0043	10.35	0.23
	HCT				**HCTTi**			
5.0	1.5918	0.0038	19.55	1.87	1.6909	0.0289	17.77	1.39
7.5	1.5918	0.0038	16.40	1.94	1.6909	0.0289	16.00	1.42
10.0	1.5918	0.0038	12.63	2.03	1.6909	0.0289	12.45	1.49
12.5	1.5918	0.0038	12.01	2.05	1.6909	0.0289	12.45	1.49
15.0	1.5918	0.0038	11.38	2.06	1.6909	0.0289	10.08	1.53

Table 6. Breaking and tensile strength of the API and API-TNT tablets

Pressing force (kN)	Breaking strength (N)	SD	Tensile strength (N)	SD	Breaking strength (N)	SD	Tensile strength (N)	SD
	DiltHCl				**DiltTi**			
5.0	24.9	1.1	0.47	0.02	69.0	1.79	1.42	0.04
7.5	53.0	3.63	1.09	0.06	96.0	2.37	2.08	0.05
10.0	66.2	4.47	1.60	3.68	122.0	4.86	2.83	0.09
12.5	104.0	4.53	2.35	0.08	142.0	2.66	3.37	0.06
15.0	124.0	3.19	2.83	0.10	156.0	2.86	3.79	0.05
	DicNa				**DicTi**			
5.0	42.9	2.64	0.85	0.05	46.0	3.04	0.93	0.05
7.5	58.1	3.68	1.21	0.08	66.0	2.80	1.44	0.05
10.0	81.2	4.58	1.74	0.07	99.0	3.63	2.27	0.08
12.5	98.1	3.91	2.17	0.08	120.0	3.30	2.83	0.07
15.0	125.0	3.00	2.73	0.07	153.0	3.05	3.80	0.06
	ATN				**ATNTi**			
5.0	79.5	2.90	1.68	0.06	102.0	4.56	1.99	0.09
7.5	82.4	2.08	1.75	0.04	121.0	1.97	2.48	0.05
10.0	89.6	1.60	1.99	0.04	138.0	2.77	2.88	0.05
12.5	101.0	4.27	2.02	0.09	141.0	2.19	3.00	0.05
15.0	102.0	3.08	2.13	0.08	149.0	4.34	3.24	0.09
	HCT				**HCTTi**			
5.0	87.0	4.20	1.63	0.08	127.0	3.16	2.65	0.07
7.5	112.0	3.84	2.18	0.07	148.0.	3.64	3.14	0.07
10.0	149.0	4.81	2.92	0.20	190.0	3.10	4.13	0.07
12.5	153.0	3.40	3.10	0.06	191.0	3.50	4.32	0.08
15.0	160.0	4.00	3.22	0.10	222.0	2.72	5.14	0.06

Table 7. Disintegration time of the API and API-TNT tablets

Compressing force (kN)	Disintegration time(min)	SD	Disintegration time(min)	SD
	DiltHCl		**DiltTi**	
5.0	0.16	0.02	0.52	0.03
7.5	0.41	0.17	2.44	0.29
10.0	8.28	0.68	9.54	0.49
12.5	11.07	1.34	15.49	0.27
15.0	18.13	0.52	18.46	0.52
	DicNa		**DicTi**	
5.0	0.20	0.01	1.34	0.09
7.5	0.41	0.05	2.13	0.05
10.0	1.05	0.13	3.21	0.41
12.5	1.58	0.19	4.26	0.65
15.0	4.23	0.05	5.27	0.37
	ATN		**ATNTi**	
5.0	1.05	0.09	4.95	0.35
7.5	1.56	0.28	9.56	0.17
10.0	3.33	0.33	13.40	0.37
12.5	5.40	0.48	15.30	0.46
15.0	6.26	0.18	18.62	0.43
	HCT		**HCTTi**	
5.0	0.12	0.02	0.31	0.06
7.5	0.18	0.03	0.48	0.16
10.0	0.23	0.06	1.18	0.13
12.5	0.23	0.06	1.43	0.07
15.0	0.28	0.03	3.19	0.30